EurJIC
European Journal of Inorganic Chemistry

A Journal of ChemPubSoc Europe

Accepted Article

Title: Iron(III) Complexes of Vitamin-B6 Schiff Base with Borondipyrromethene Pendants for Lysosome Selective Photocytotoxicity

Authors: Akhil Chakravarty, Somarupa Sahoo, Santosh Podder, Aditya Garai, Shamik Majumdar, Nandini Mukherjee, Uttara Basu, and Dipankar Nandi

To be cited as: *Eur. J. Inorg. Chem.* 10.1002/ejic.201701487

Link to VoR: http://dx.doi.org/10.1002/ejic.201701487

WILEY-VCH

10.1002/ejic.201701487

WILEY-VCH

Iron(III) Complexes of Vitamin-B_6 Schiff Base with Borondipyrromethene Pendants for Lysosome Selective Photocytotoxicity

Somarupa Sahoo,[a] Santosh Podder,[b] Aditya Garai,[a] Shamik Majumdar,[b] Nandini Mukherjee,[a] Uttara Basu,[a] Dipankar Nandi*[b] and Akhil R. Chakravarty*[a]

Dedication ((optional))

Abstract: Iron(III) complexes of a vitamin B_6 Schiff base and *NNN*-donor ligands with pendant borondipyrromethene (BODIPY) moieties, *viz.* $[Fe(L^{1\text{-}3})(L^{4,5})](NO_3)$ (**1-4**), where L^1 is benzyl-bis((pyridin-2-yl)methyl)methanamine (bzdpa in **1**), L^2 is a non-iodinated BODIPY appended dipicolylamine ligand (in **2**, **3**), L^3 is the diiodinated-BODIPY analogue in **4**, L^4 is vitamin B_6 Schiff base, *viz.* 3-hydroxy-5(hydroxymethyl)-4-(((2-hydroxyphenyl)imino)methyl)-2-methylpyridine (in **1, 3** and **4**) and L^5 is 2-[(2-hydroxyphenylimino)-methyl]phenol (in **2**) as a non-pyridoxal Schiff base, were prepared, characterized and their cellular localization and cytotoxic activity in light and dark were studied. The diiodo-BODIPY complex **4** displayed remarkable photo-induced cytotoxicity in visible light (400-700 nm) with IC_{50} values within 0.11 to 0.25 μM and ~200-fold lower dark toxicity. Complex **3** being fluorescent was used for cellular imaging by confocal microscopy. Complex **4** showed supercoiled pUC19 DNA cleavage activity via generation of singlet oxygen ($^1O_2$) as the reactive oxygen species (ROS). Selective uptake of the complexes was observed from competitive cellular incorporation assays in cancer and non-cancerous cells. The complexes also showed no apparent toxicity up to 100 μM in the immortal human lung epithelial cells HPL1D in both light and dark. Complex **3** showed preferential accumulation in the lysosomes giving a Pearson's correlation coefficient value of ~0.7.

Introduction

Two important aspects in designing an anticancer drug are: (i) the selectivity of the drug between normal versus cancer cells and (ii) specific localization of the drug to a particular cellular organelle in preference to the others. To achieve the first objective, several bioactive organic molecules are being used in conjugation with the main drug to drive it specifically to the cancer cells.[1] This significantly enhances the efficacy of the drug and reduces the drug and dose related toxicity. For instance, Frochot *et al.* have used glycosylated and folic acid conjugated photosensitizers for selective cytotoxicity.[2] Low and coworkers have developed receptor based targeted therapeutic agents showing better activity.[3] Vitamin B6 (VB_6) is one such molecule which plays an important role in cellular processes by acting as a cofactor.[4] Cellular uptake of VB_6 is by means of diffusion, through specific transporting membrane carriers known as Vitamin Transport Channels (VTC).[5] During the uncontrolled cell proliferation in cancer, the activity of Serine Hydroxymethyltransferase (SHMT) increases manifold as it aids in the biosynthesis of DNA, which also leads to an increased requirement of VB_6.[6] Therefore, it is assumed that a molecule conjugated with this moiety will have significant cellular uptake, thus enhancing its selectivity and efficacy. We have earlier used this molecule to target cancer cells selectively.[7,8] Iron being a bioavailable metal present in human body in various enzymes and receptors is chosen for our study to make covalent conjugates with organic moieties that are selected for desired activity. Iron reduces the metal related toxicity that can arise in case of leaching.[9] The clinical success of iron-bleomycins as chemotherapeutic agents showing oxidative damage of DNA by forming cytotoxic hydroxyl radicals provides impetus in using this metal for cancer treatment and cure.[10] Metal complexes having ligands with a VB_6 moiety are expected to show significant enhancement in the cellular uptake compared to the control species lacking such a moiety. BODIPY dyes are a versatile class of photosensitizers that exhibit properties such as high molar extinction coefficient in the absorption band, sharp emission bands with minimal Stokes shift, high resistance to photo-bleaching and readily amenable for structural modification. This makes them an appropriate choice for cellular imaging and exploiting their light-induced ROS generation ability for cytotoxicity study.[11] Research on using these dyes to generate singlet oxygen by photo-irradiation has received major attention in recent years. Akkaya *et al*. have worked extensively in using BODIPY dyes as photodynamic therapy (PDT) agents.[12] The present work stems from our interest in designing new ternary iron(III) complexes with VB_6 incorporated in the Schiff base framework that are expected to give higher cellular uptake in cancer cells over normal cells.

The other important aspect is the specific localization of the drug to a particular cellular organelle. Cisplatin and its analogues are known to localize in the nucleus and bind to nuclear DNA.[13] The low efficacy of some of these chemotherapeutic drugs is attributed to the nuclear excision repair (NER) mechanism which is operative for nuclear DNA.[14] Cisplatin is also known to show poor selectivity between normal versus cancer cells. PDT has emerged as an alternative Food and Drug Administration (FDA) approved therapeutic approach to treat cancer.[15] This methodology is useful for selective treatment of tumors by the drug Photofrin® which as a

[a] Somarupa Sahoo, Dr. Aditya Garai, Nandini Mukherjee, Dr. Uttara Basu, Prof. Akhil R. Chakravarty
Department of Inorganic and Physical Chemistry
Indian Institute of Science, Bangalore 560012, Karnataka, India
E-mail: arc@iisc.ac.in; http://ipc.iisc.ac.in/~arc/index.html
[b] Santosh Podder, Shamik Majumdar, Prof. Dipankar Nandi
Department of Biochemistry
Indian Institute of Science, Bangalore 560012, Karnataka, India
E-mail: nandi@iisc.ac.in; http://biochem.iisc.ernet.in/dpnLab/

Supporting information for this article is given via a link at the end of the document.

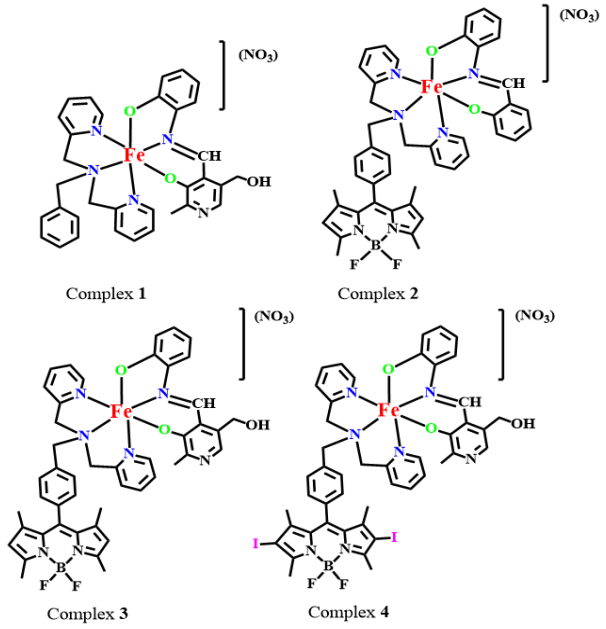

Figure 1. Iron(III) complexes **1-4** as their nitrate salts.

photosensitizer generate singlet oxygen ($^1O_2$) as the reactive oxygen species (ROS) on exposure to red light of 633 nm.[16] This PDT drug shows better selectivity with its localization in the mitochondria of the cells. The advantage of PDT over conventional chemotherapy is based on this selectivity in which the light-exposed cancer cells are only damaged thus leaving the unexposed healthy cells unaffected. The current focus lies on developing targeted drugs with minimal side effects. Photoactive metal-based coordination complexes with versatile structural diversity and biophysical properties are reported to show promising results in targeting mitochondria.[17] Gasser *et al.* have reported ruthenium complexes showing anticancer activity by localizing in the lysosomes.[18] Dhar *et al.* have also demonstrated enhanced activity of mitochondria targeting platinum complexes, while Neamati *et al.* have shown that the anticancer activity of chlorambucil results from its mitochondrial localization.[19,20] Sadler *et al.* have suggested that preferential localization could be an important aspect of current and future anticancer drug design.[21]

Combining the above mentioned strategies of targeting cancer versus normal cells and with the knowledge that borondipyrromethene (BODIPY) based photosensitizers prefer mitochondrial localization[22,23], we have designed and synthesized new ternary iron(III) complexes of formulation $[Fe(L^{1\text{-}3})(L^{4,5})](NO_3)$ (**1**-**4**), where L^1 is benzyl-bis((pyridin-2-yl)methyl)methanamine (bzdpa in **1**), L^2 is non-iodinated BODIPY-appended dipicolylamine ligand (in **2**, **3**), L^3 is diiodinated-BODIPY analogue (in **4**), L^4 is vitamin B6 Schiff base, *viz.* 3-hydroxy-5-(hydroxymethyl)-4-(((2-hydroxyphenyl)imino) methyl)-2-methylpyridine (in **1**, **3** and **4**) and L^5 is 2-[(2-hydroxyphenylimino)-methyl]phenol) (in **2**) as a non-pyridoxal Schiff base (Figure 1). While vitamin B_6 unit is expected to facilitate the uptake of the complex selectively into the cancer cells over the normal cells, the BODIPY-appended *NNN*-donor dipicolylamine (dpa) ligand in the ternary structure in complex **4** is expected to generate singlet oxygen causing light-induced cell death by type-II pathway that is known for Photofrin®. Complex **3** contains a highly emissive BODIPY unit which can be used for cellular imaging to identify the target organelle for these complexes. Complex **2** contains a salicylaldehyde Schiff base instead of vitamin B_6. This complex is used to study the cancer cell vs normal cell selectivity of the complexes as imparted by the vitamin moiety. And finally, complex **1** which is devoid of any photosensitizing group is used as a control to ascertain the photosensitizing ability of the BODIPY moieties.

The significant results of this work include: (i) higher cellular uptake in the cancer cells than in normal cells, (ii) remarkable PDT activity in light of 400-700 nm with singlet oxygen mediated apoptotic cell death, and (iii) significant localization of the complex in the lysosome instead of the anticipated mitochondria. This observation is serendipitous as lysosome localizing PDT agents are rare in the literature.[24-28] Tsubone *et al.* in a recent paper have demonstrated that lysosome-specific photo-damage results in enhanced activity by using new porphyrin dyes.[24] The enhanced activity is ascribed to the lysosomal membrane damage and induction of autophagy-associated cell death. Iron oxide based magnetic nano particles were reported to target cancer cells via overexpressing the epidermal growth factor receptor (EGFR) that were found to be permeable in the lysosomal membrane when an alternating magnetic field was applied.[25] BODIPY based systems that target lysosomes are also being studied recently.[26] Peng *et al.* have reported lysosome-targeted BODIPY dyes showing PDT activity.[27] The present work exemplifies the first metal-based photo-cytotoxic agent showing light-induced cell death on localizing to this important cellular organelle which is involved in cellular protein degradation.[28] Herein we report the synthesis, characterization and photo-induced anticancer activity of the iron(III) complexes **1**-**4**.

Results and Discussion

Synthesis and Chemical Characterization

The salicylaldehyde (H_2L) and pyridoxal hydrochloride containing tridentate Schiff bases and the dipicolylamine (dpa) ligands L^2 and L^3 with appended BODIPY moieties were prepared by reported procedures.[29] Iron(III) complexes **1-4** were prepared in good yield following general synthetic procedure in which $FeNO_3.9H_2O$ was initially reacted with the dipicolylamine ligand in 1:1 molar equivalent in anhydrous methanol (**1**, bzdpa; **2** and **3**, L^2; and **4**, L^3) with a subsequent addition of the deprotonated Schiff base ligand using triethylamine in methanol. (Scheme S1) The product was isolated as nitrate salt and the complexes were characterized by spectroscopic and analytical methods. Selected physicochemical data are given in Table 1. Complex **1**, without having any BODIPY unit, was used as a control due to its inactivity in light. Complex **2** lacking the pyridoxal Schiff base was also used as a control to probe the selective cellular uptake of the VB_6 containing complexes. Complexes **3** and **4** having the pendant BODIPY moieties were used for cellular imaging and photo-induced cytotoxicity study. Complex **3** for its fluorescent properties was used for

Table 1. Selected physicochemical and ct-DNA binding data of the complexes **1** - **4** as their nitrate salts.

Complex	λ_{max}[a]/nm [ε/(M^{-1} cm^{-1})]	λ_{em}[b]/ nm [Φ_F]	E_{pc}[c] (V)	μ_{eff} [d]	Λ_M [e] / (S m^2 M^{-1})	K_b [f] (M^{-1})
1	270 (46450), 386 (16025)	470 (-)	-0.63	5.86	77	9.45 x 10^4
2	400 (26420), 500 (42400)	560 (0.12)	-0.45	5.83	69	-
3	265 (42130), 500 (45100)	560 (0.12)	-0.49	5.82	71	7.83 x 10^5
4	407 (25140), 532 (35520)	560 (0.01)	-0.44	5.85	73	4.99 x 10^5

[a] Visible bands within 400-700 nm in 1:1 DMF–DPBS buffer. [b] In 10% aqueous DMSO. Quantum yield [Φ_F] was measured using fluorescein as the standard (Φ_F = 0.79). [c] E_{pc} is the cathodic peak potential of the Fe(III)/Fe(II) redox couple vs. SCE in 5 mL DMF-0.1 M TBAP, 2.0 mmol of the complexes. The scan rate was 100 mV s^{-1}. [d] μ_{eff} in μ_B for solid samples of the complexes at 25 °C. [e] Λ_M, molar conductivity in S m^2 M^{-1} in 10% aqueous DMF at 25 °C. [f] Intrinsic ct- DNA binding constant (ct, calf thymus).

cellular imaging to probe any organelle selective localization of the complex. It is known that BODIPY moieties without heavy atoms like Br or I do not generate significant singlet oxygen ($^1O_2$) as the ROS.[30] Complex **4** with its diiodoBODIPY unit as a photosensitizer was hence used for the PDT activity. The complexes gave the elemental analysis data in accordance to the ternary complex formulation. They were soluble in methanol, ethanol, dimethyl sulfoxide and dimethylformamide (DMF). The BODIPY ligands alone were soluble in halogenated solvents, however, the solubility reduced upon binding to iron(III). They were insoluble in hydrocarbons like hexane, toluene and benzene. The complexes were 1:1 electrolytes in DMF giving molar conductivity values in the range of 70-80 S m^2 M^{-1}. The mass spectra of the complexes showed single $[M]^+$ peak in methanol suggesting the monomeric nature of the ternary complexes (Figures S1-S4). The IR spectra showed characteristic bands for nitrate anion at ~1450 cm^{-1} and for the C=C and C=N stretching in the range of 1500 to 1700 cm^{-1} (Figure S5).[31] The complexes were five-electron paramagnetic with magnetic moment values of ~5.8 μ_B at room temperature indicating high spin state of the iron(III) center.

Photophysical and Photochemical Characterization

The two phenolic groups present on the Schiff base ligands stabilize the metal in its high-spin +3 oxidation state due to their strong binding affinity for the metal. This observation is important as a stable complex reduces the possibility of metal leaching in the biological medium. Hence, the metal-bound state of the complexes was monitored by absorption spectroscopy in 1:1 v/v DMSO:DPBS (DPBS: Dulbecco's phosphate buffered saline) medium up to 36 h to observe any changes in the spectral band intensity. The intensity remained marginally diminished in the cell incubation window of 4 h for complexes **2**-**4**. The diiodo-BODIPY complex **4**, however, showed decrease in intensity after 12 h, possibly due to instability of the diiodo-BODIPY moiety. The time dependent absorption spectra for free ligands and complexes **2-4** are given in Figures S9, S10.

The UV-visible spectra of the complexes **2**-**4** in 1:1 (v/v) DMF:PBS (PBS, phosphate buffered saline) medium showed an

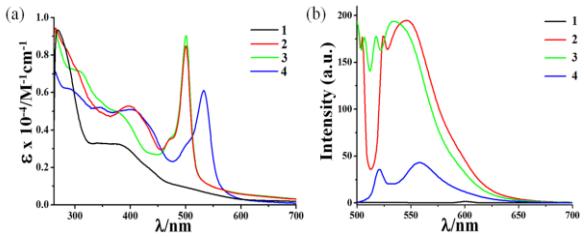

Figure 2. (a) Absorption spectra of the complexes **1**-**4** in 1:1 (v/v) DMSO:DPBS buffer medium. (b) Emission spectra of the complexes **1**-**4** in 10% aqueous DMSO (λ_{ex}: 300 nm for **1**; 480 nm for **2** and **3**; 520 nm for **4**).

intense π→π* transition arising from the BODIPY and diiodo-BODIPY units at 500 and 532 nm, respectively.[32] A ligand to metal charge transfer (LMCT) band was seen at 400 nm for the phenolate π orbital to the dπ* orbital of iron.[33] The dpa ligand showed π→π* band in these complexes at ~280 nm. Complex **3** with the BODIPY unit was highly emissive in 10% aqueous DMSO upon excitation at 480 nm (Figure 2). This complex was found to be suitable for cellular imaging studies by confocal imaging with its fluorescence quantum yield (Φ_F) value of 0.12. Complex **4** was found to be non-emissive with Φ_F value of 0.01 (fluorescein in 0.1 M NaOH used as standard). The iodine atoms seemed to facilitate intersystem crossing (ISC) via heavy atom effect, hence making it suitable for photodynamic therapy (PDT). Complexes **3** and **4** gave singlet oxygen quantum yield values of 0.11 and 0.56, respectively, when estimated using Rose Bengal as a standard (Figure S11). The complexes were redox active showing a quasi-reversible Fe(III)-Fe(II) couple near -0.45 V versus SCE (saturated calomel electrode) in DMF - 0.1 M TBAP (tetrabutylammonium perchlorate). Reduction peaks from the BODIPY unit and the Schiff base were visible near -1.2 V. No oxidative response was observed in the complexes in anodic scans (Figures S6, S7). Such a low redox potential for the Fe(III)/Fe(II) couple makes the complexes inactive as "chemical nucleases" in the presence of cellular thiols, *viz*. glutathione, thus reducing their cellular dark toxicity.[10]

Theoretical Studies

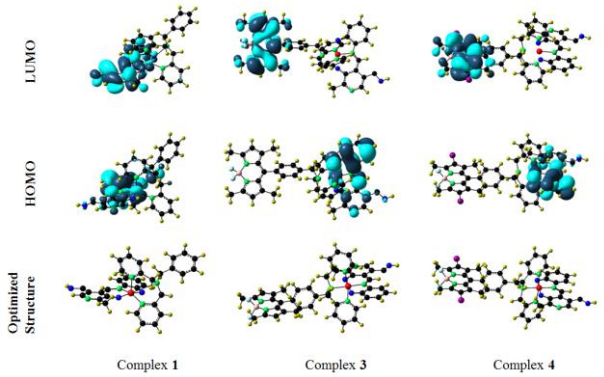

Figure 3. Geometrically optimized structures of the complexes **1**, **3** and **4** obtained from DFT.

The energy optimized structures of the complexes **1**, **3** and **4** were obtained by density functional theory (DFT) using B3LYP with LanL2DZ basis set for all atoms with Gaussian 09 software package to probe the electronic nature of the complexes.[34] The optimized structures and the HOMO-LUMO are shown in Figure 3. The frontier molecular orbital (FMO) diagram for **1** suggests the presence of both HOMO and LUMO on the Schiff base moiety. In complexes **3** and **4**, the LUMO was based on the BODIPY appended dipicolylamine moiety while the HOMO lies on the Schiff base-metal unit, which gives rise to the metal to phenolate ligand-to-metal charge transfer (LMCT) transition that was observed near 385 nm in the UV-visible spectra. The participation of the BODIPY core in forming the FMOs is evident as a photosensitizing unit in the complex. The energy difference between LUMO and HOMO for the complexes is in the range of 2.3 to 2.5 eV.

Photocytotoxicity

The antitumor activity of the complexes in light (visible light source of 400–700 nm; Luzchem photoreactor, 10 *J* cm^{-2}; irradiation time of 1 h) and dark was studied using cell viability assay in three cancerous cell lines, *viz.* HeLa, (human cervical cancer), MCF-7 (human breast cancer) and HepG2 (human liver carcinoma cells) and one non-cancer immortalized cell line, *viz.* HPL1D (transformed human epithelial lung cells). The complexes were administered into the cells as a 1% DMSO solution. They were first prepared in DMSO and the final volume was adjusted to 1% by further dilution with reconstituted DMEM medium (10% FBS) in which the cells were cultured. The complexes were incubated for 4 h in dark and then one batch was irradiated with visible light, while the other was kept in dark. Cytotoxicity was measured from the IC_{50} values (50% inhibitory concentration) obtained from the cell viability assay. The complexes generally showed significant photocytotoxicity in the cancerous cell lines and were negligibly toxic in dark conditions (Table 2, Figures S12-S16).[35-40] The IC_{50} values of the control complex **1** in light of 400-700 nm were >100 μM in all the cell lines. The same for complex **3** was significantly low (~4.0 μM) due to the presence of the photosensitizing BODIPY unit. The values reduced even further to nanomolar range (~0.15 μM) for the diiodo-BODIPY complex **4** due to high quantum yield of singlet oxygen as the ROS. Complexes **2** and **3** remained essentially non-toxic in HPL1D cells (Figure S12 for cumulative depiction of the IC_{50} values). This selective toxicity of the complexes towards cancer cells over the non-cancerous cells can be attributed to their enhanced cellular uptake in the cancer cells due to vitamin-B6 moiety and high photosensitizing ability of the diiodo-BODIPY unit in visible light.

Cellular uptake

To investigate whether the VB_6 moiety possessed any selective role in facilitating the uptake of the complexes into the cancer cells over the normal cells, flow cytometry based cellular incorporation assay was performed using the fluorescent-VB_6 containing molecule **3** and its non-vitamin analogue **2**. A dose-dependent as well as competitive uptake study along with time dependent analysis were performed in HeLa and HPL1D cells (Figure 4). The data demonstrated that HeLa cells have a preferential uptake of complex **3** as compared to **2** within an incubation time of 4 h. No such difference was observed in the HPL1D cells. Interestingly, VB_6 did not assist in quicker ingestion of the drug moiety in HPL1D cells, which was evidenced by varying the incubation time from 2 to 4 h in complex **3**. It showed the same amount of uptake at both time points in HPL1D cells. However, there was a significant difference in the uptake of **3** in HeLa cells, suggestive of higher uptake in cancer cells owing to their increased demand for VB_6 as a nutrient.[41] In addition to that, there was an increase in the uptake of the complex into the HeLa cells with the increase in incubation time (Figure S17). Complete incorporation was noteworthy in HeLa cells upon 4 h post- incubation in all the three doses used. This might be due to the selective uptake of the complex by transporter channels initially and subsequent internalization via simple diffusion with the passage of time. This observation helped us to standardize

Table 2. IC_{50} (μM) values of the complexes **1**-**4** and other relevant compounds

Compound	HeLa		MCF-7		HEPG2		HPL1D	
	D	L[a]	D	L[a]	D	L[a]	D	L[a]
1	> 100	>100	> 100	> 100	> 100	> 100	>100	>50
2	> 100	12.2 ± 1.1	> 100	12.1 ± 1.4	> 100	10.3 ± 1.3	>100	>50
3	> 100	5.5 ±1.2	> 100	3.25 ± 0.08	> 100	3.9 ± 0.6	>100	>50
4	> 100	0.11 ± 0.08	> 100	0.20 ± 0.04	> 100	0.22 ± 0.01	>100	>50
[Fe(bpyag)(pyap] (NO_3)[b]	> 80	8.2 ± 0.6						
[Fe(cat)NO_3][c]	>100	6.2 ± 0.1						
[Fe(BHA)(pydpa)Cl]Cl[d]	>100	14.6 ± 0.7						
[Fe(pybpa)(L)](NO_3)[e]	3.3± 1.1							
Photofrin[f,g]	>41	4.3 ± 0.2						

[a] Visible light of 400–700 nm (10 J cm^{-2}). The IC_{50} values of the Schiff base ligands in HeLa cells were >100 μM in both light and dark. The cell viability assay of the BODIPY appended dipicolylamine bases could not be done due to their poor solubility. [b] bpyag is N,N-bis(2-pyridylmethyl)-2-aminoethyl-β-D-glucopyranoside and H_2pyap is 3-(2-hydroxyphenylimino)-1-pyrenylbutan-1-one.[35] [c] L is 9-[(2,2'-dipicolylamino)methyl]anthracene.[36] [d] BHA is benzhydroxamate and pydpa is (pyrenyl)dipicolylamine.[37] [e] pybpa is (pyren-1-yl)-N,N-bis((pyridin-2-yl)methyl)methanamine and (H_2L is 3-hydroxy-5-(hydroxymethyl)-4-(((2-hydroxyphenyl)imino)methyl)-2methylpyridine.[29 a] [f] The values are taken from Ref 38 and Ref 39 and converted to μM using the approximate molecular weight of Photofrin as 600 g mol^{-1}. At 633 nm excitation with fluence rate of 5 J cm^{-2}. [g] Cisplatin shows an IC_{50} value of 13.0±1.2 in HeLa, 2.0±0.3 in MCF 7 and 7.23 ± 0.04 in HepG2 cells.[40]

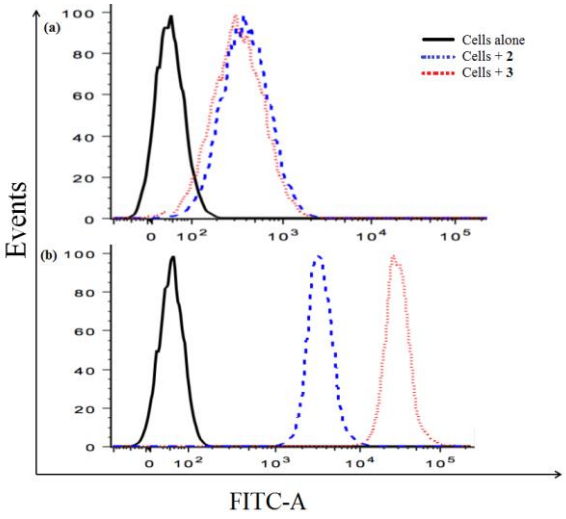

Figure 4. Histogram depicting cellular incorporation of complex **2**, i.e. the non-vitamin analogue in blue dotted line and complex **3**, which contains the VB_6 moeity in red dotted line in (a) HPL1D and (b) HeLa cells post 4 h of incubation at 37°C. Complex concentration: 2 μM.

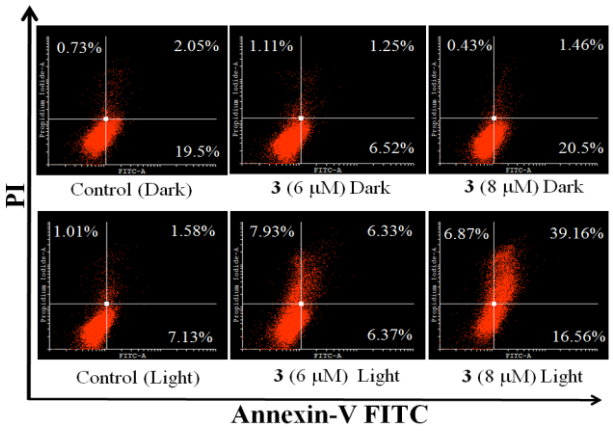

Figure 5. Annexin-V-FITC/PI assay showing the percent population of early apoptotic cells stained by Annexin-V-FITC alone (lower right quadrant), dead cells stained by propidium iodide alone (upper left quadrant), and late apoptotic cells stained by both Annexin-V-FITC and PI (upper right quadrant) in HeLa cells alone or treated with complex **3** in the dark or after exposure to visible light for 1 h (400− 700 nm).

the incubation time of the complexes for other *in-vitro* studies prior to light irradiation.

The VTC mediated uptake of the drug was also studied by pre-saturating the cells with 4 mM VB_6 (pyridoxal hydrochloride) for 1 h prior to the addition of complex **3** so that the channels are blocked by the externally added VB_6. HeLa cells demonstrated a noticeable difference in uptake of the complex with and without pre-saturation as compared to that with the normal cells (Figure S18).

Quantification of Cellular Iron by ICPMS

The results obtained from the incorporation studies showed a differential uptake of complexes **2** and **3** in the cancer cells. To ascertain this observation, the iron content inside the cells was measured by the ICPMS (Inductively Coupled Plasma Mass Spectroscopy) method.

The cells were incubated with complexes **2** and **3** in dark and the iron content was measured after an incubation period of 4 h. Intracellular iron content was recorded to be 21 and 127 ng/L × 10^5 cells, for complexes **2** and **3**, respectively. Thus, the cells treated with complex **3** showed about 6 times higher iron content than the non-vitamin analogue **2**. This observation also correlated to the enhanced cytotoxicity seen for complex **3** despite having the same photosensitizing unit L^2. This further strengthens the argument of selective internalization of the complex due to the appended vitamin B6 moiety.

Annexin-V / FITC- PI Assay

Apoptotic cell death was evaluated using Annexin V- fluorescein isothiocyanate (FITC)/ Propidium Iodide (PI) method. Annexin V is a cellular protein which binds to the phophatidylserine, a glycerophospholipid component of the cell membrane. Exposure of this protein on the external surface of the plasma membrane is considered as a hall mark feature of apoptosis and forms the basis for the Annexin V (conjugated to a fluorescent dye FITC emitting at 470 nm) binding assay to determine apoptotic cell death by flow cytometer. PI is a membrane impermeant dye which emits red at 617 nm. It is excluded from viable cells and used as the second fluorescent marker to detect necrotic cells.

The cells, pretreated with 0.1 μM of complex **4**, were stained with Annexin-V FITC and PI and then studied in dark and after photo-irradiation. Complex **4** exhibited ~19% of cell population in the late apoptotic stage with just 30 min irradiation. The irradiation time could not be extended any longer as the complex (IC_{50} in nanomolar range) was highly phototoxic and sufficient live cells were not available for FACS analysis on delaying the same. The population of cells undergoing necrosis (stained with PI) was significantly low suggesting the overall apoptotic mode of cell death. The cells were then treated with two concentrations of the relatively less active complex **3** (6 and 8 μM) followed by irradiation with visible light (400–700 nm) for 1 h. On performing this assay with 4 h post photo-irradiation, about 15% cells were seen in the Q2 and Q3 (Q = quadrant) which is indicative of early and late apoptosis respectively. With a slightly increased concentration, this value rose up to ~55% with a negligible necrotic population (Figure 5, Figure S19). The data established the highly photocytotoxic properties of complexes **3** and **4**.[42]

Reactive Oxygen Species (ROS)

ROS is one essential requirement for PDT in inducing cell death *via* apoptosis. BODIPY dyes produce singlet oxygen as the ROS upon photo-activation. Complex **4** was probed by DCFDA (2',7'-dichlorofluorescien diacetate) assay for the generation of any ROS in HeLa cells on exposure to light (400-700 nm) at IC_{50}

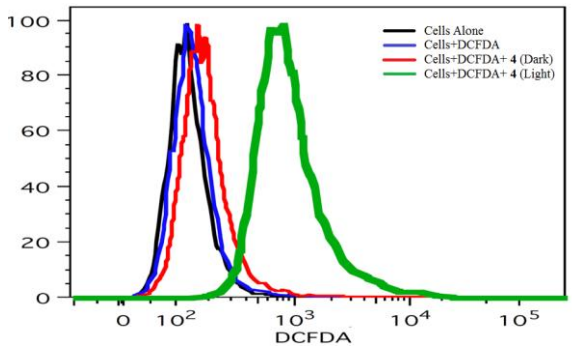

Figure 6. Flow cytometric analysis showing ROS generation by complex **4** in the dark and upon visible light irradiation in HeLa cells. Greater positive shift in fluorescence of DCF indicates greater extent of ROS generation in visible light (400-700 nm).

concentration. Cellular ROS oxidizes DCFDA to 2',7'-dichlorofluorescien (DCF) which upon excitation at 488 nm emits at 525 nm. The emission intensity of DCF was quantified by flow cytometry giving an indirect estimate of the ROS generation. Untreated cells did not show any DCF fluorescence, while significant shift in the spectra was observed for complex **4** on light exposure indicating formation of ROS. This was not observed in dark, marking the lack of ROS in the absence of light exposure (Figure 6). Since two kinds of ROS, i.e. singlet oxygen via a type-II process or hydroxyl radicals via photo-redox pathway could be generated in the PDT process, the true nature of ROS was ascertained by DPBF (diphenylisobenzofuran) assay and pUC19 DNA photocleavage activity.[43] DPBF forms endoperoxides upon reaction with singlet oxygen that leads to the quenching of its absorbance at 414 nm.[44] An earlier report from our lab showed that the diiodinated BODIPY ligand L^3 itself has a singlet oxygen quantum yield (Φ_Δ) of 0.8.[45] An indirect estimation of the same using Rose Bengal as the standard (Φ_Δ = 0.76 in DMSO)[46] gave a Φ_Δ of 0.56 for complex **4** and 0.11 for complex **3**.

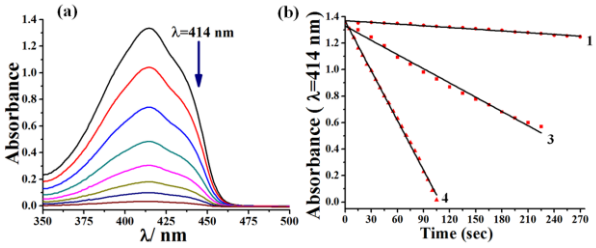

Figure 7. (a) Absorption spectral traces of diphenylisobenzofuran (DPBF) and complex **4** (0.1 μM) in DMSO on exposure to light (400–700 nm, 10 $J.cm^{-2}$) for exposure time of 5 sec. (b) Plot showing changes in absorbance of DPBF at 414 nm with time on light exposure with complexes **1**, **3** and **4**. The slope gives an indication of the amount of singlet oxygen generated with higher slope meaning greater singlet oxygen generation.

Following this observation, a 70 μM solution of DBPF was treated with 2 μM solution of the complexes **1, 3** and **4** and the absorbance band intensity was monitored at 5 sec intervals of photo-irradiation with visible light of 400-700 nm (Luzchem photoreactor). Complex **4** caused a complete depletion of the absorption intensity within 120 sec of photo-irradiation. The ROS generation ability followed the sequence: **4** > **3** >> **1** (Figure 7, Figure S20). Complex **1** having no photoactive moiety did not show any significant singlet oxygen generation. The DPBF absorption decay rate for complex **4** was found to be 13.5 x 10^{-3} sec^{-1} which was 4 fold higher than that for complex **3** (4 x 10^{-3} sec^{-1}) and 12 fold higher than complex **1** (0.36 x 10^{-3} sec^{-1}).

Cellular Localization

The localization of complex **3** (fluoresces in green) was monitored in HeLa cells by means of confocal microscopy. The cells were treated with 5 μM of the complex and incubated for 4 h in dark. The complex showed no apparent localization in the nucleus and accumulated primarily in some portions of the cytoplasm. Co-localization studies with Mito-tracker red (MTR) and Propidium Iodide (PI) showed no significant accumulation of the complex either in mitochondria (PCC = ~0.3) or in the nucleus (PCC= ~0.1). Co-staining with Lyso-Tracker Red gave a Pearson's correlation coefficient (PCC) value of ~0.7 suggesting a positive co-localization of complex **3** with Lyso-Tracker (LTR) (Figure 8).

This is an interesting observation as targeting lysosomes can initiate the apoptotic process in cell death.[47] Lysosomes as "suicidal bags" in the cells contain enzymes to break down the worn out organelles and other biomolecules. Like the mitochondria, lysosomes are the attractive targets for initiating anticancer activity.[48] Lysosomal membrane permeabilization (LMP) can be triggered by damaging the lysosomes leading to proton and hydrolase leakage. Specifically, it has been suggested that the intracellular release of cathepsins into the cytosol by LMP can activate the intrinsic apoptotic pathway inducing cell death *via* apoptosis.[49].

DNA Cleavage and Mechanistic Aspects

The DPBF experiments showed singlet oxygen as the generated ROS by the complexes. To rule out the possibility of formation of any radical based ROS, the mechanistic aspects of the plasmid pUC19 DNA photo-cleavage reactions were studied in the presence DABCO (1,4-diazabicyclo[2.2.2]octane), NaN_3 and TEMP (2,2,6,6-tetramethylpiperidine) as singlet oxygen quenchers, and KI and DMSO as hydroxyl radical scavengers, catalase as a H_2O_2 scavenger, and superoxide dismutase (SOD) as a superoxide radical scavenger.[37] The binding interaction of the complexes with calf thymus (ct) DNA was studied in 5% DMF-Tris buffer (pH = 7.2) by UV-Vis absorption method (Figure S21). The "chemical nuclease" activity of the complexes was studied in the presence of glutathione (GSH) as a reducing agent and H_2O_2 as an oxidizing agent (Figures S22, S23).

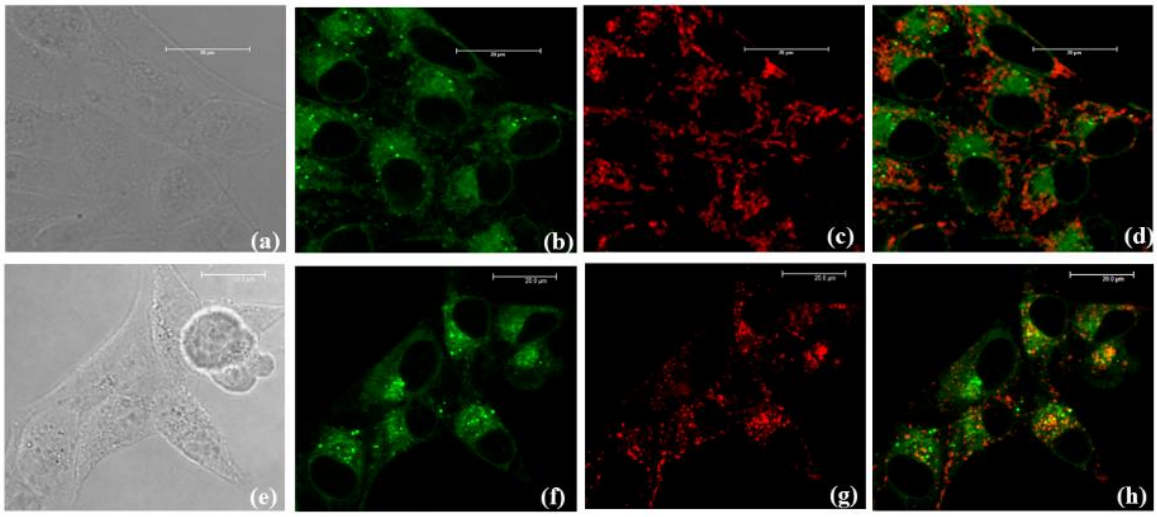

Figure 8. Confocal microscopic images of HeLa cells after 4 h incubation with complex **3**: panels (a) and (e) are bright field, panels (b) and (f) are for the fluorescence of complex **3**, panels (c) and (g) are for fluorescence of Mito-Tracker Deep Red and Lyso-Tracker Deep Red respectively , panel (d) shows the merged image of (b) and (c), and panel (h) shows the merged image of (f) and (g).

The intrinsic binding constant (K_b) values of the complexes were determined from the absorption spectral traces of complexes **1, 3** and **4** in 5 mM Tris-HCl buffer (pH 7.2) by increasing the quantity of calf thymus DNA. The K_b values varied as: **3** ≅ **4** >> **1**. The DNA cleavage properties were studied by using supercoiled (SC) pUC19 DNA on photo-irradiation with a green light source (532 nm) to excite the BODIPY band. The gel diagram showed significant photo cleavage of DNA in green light by both **3** and **4** (25 μM). Complexes **2** and **3** showed the formation of ~65% of nicked circular (NC) DNA, while complex **4** showed ~87% cleavage of SC DNA. The control complex, without the BODIPY unit, showed ~6% SC DNA photo cleavage. No apparent cleavage of DNA was observed when the samples were not photo-exposed. The DNA photo-cleavage activity of complex **4** reduced to only ~15% from 87% in presence of singlet oxygen quenchers, while the hydroxyl and SOD scavengers did not show any apparent effect, suggesting singlet oxygen as the only ROS (Figure 9, Figure S24). D_2O as solvent enhanced the cleavage activity as it increases the lifetime of singlet oxygen.[50] The iron(III) complexes were "chemical nuclease" inactive due to stabilization of the metal in its trivalent oxidation state. The results indicate that PDT activity of the diidoBODIPY complex **4** is due to singlet oxygen as the ROS.

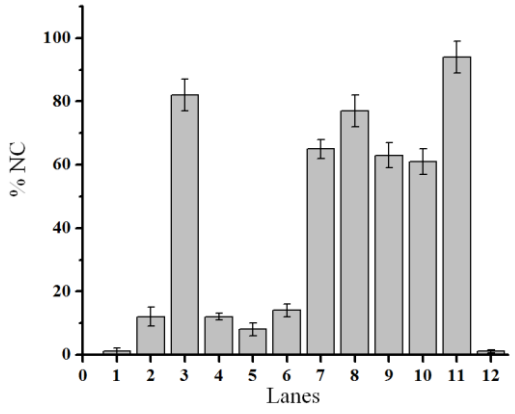

Figure 9. Bar diagram showing the mechanistic aspects of supercoiled (SC) pUC19 DNA photo-cleavage activity of the diiodoBODIPY complex **4** (25 μM), in the presence of various singlet oxygen quenchers and radical scavengers under irradiation with diode laser light of 532 nm (100 mW, 75 min exposure, lanes 3-12) in the form of %NC DNA (NC, nicked circular): lane 1: DNA alone; lane 2: DNA + **4** (Dark); lane 3: DNA + **4** (Light); lane 4: DNA + **4** + TEMP (0.5 mM); lane 5: DNA + **4** + DABCO (0.5 mM); lane 6: DNA+ **4** + NaN_3 (0.5 mM); lane 7: DNA + **4** + SOD (superoxide dismutase , 4 units); lane 8: DNA + **4** + DMSO (4 μL); lane 9: DNA + **4** + KI (0.5 mM); lane 10: DNA + **4** + catalase (4 μL); lane 11: DNA + **4** + D_2O (16 μL); lane 12: DNA + **4** + Argon.

Conclusions

Ternary iron(III) complexes having Schiff base with cell targeting Vitamin-B6 moiety and dipicolylamine bases with appended photoactive BODIPY units were prepared and their cellular activities were studied. The complexes having VB_6 moiety showed selective incorporation into the cancer cells than immortalized transformed cells. Moreover, the complex with a diiodo-BODIPY moiety exhibited excellent PDT activity in visible light (400−700 nm), while remaining essentially non-toxic in dark. The ROS generated during the PDT process was ascertained to be singlet oxygen while the mode of cell death was apoptosis. The present VB_6 derivative Schiff base complexes were seen to localize in the lysosomes, which makes them an effective tool to avoid nuclear excision repair (NER) process associated with the nuclear DNA causing drug resistance of the currently used platinum-based chemotherapeutic drugs. The present BODIPY complexes exemplify the metal-based PDT agents showing apoptotic cell death by targeting lysosomes instead of the anticipated mitochondria of the cancer cells. The diiodo-BODIPY

complex satisfies all the major criteria of PDT thus making it suitable for further studies for potential *in vivo* applications.

Experimental Section

Materials and Methods: The reagents and chemicals were obtained from the commercial sources, *viz*. S. D. Fine Chemicals, India, Invitrogen, USA and Sigma–Aldrich, U.S.A. Solvents used were purified by standard methods.[51] The complexes were prepared under nitrogen atmosphere. Plasmid supercoiled (SC) pUC19 DNA (cesium chloride purified) was procured from Bangalore Genie (India). Tris(hydroxymethyl)aminomethane-HCl (Tris-HCl) buffer (pH = 7.2) was prepared using deionized and sonicated double distilled water for DNA work. 3-(4,5-Dimethylthiazol-2-yl)-2,5-diphenyltetrazolium bromide (MTT), Dulbecco's Modified Eagle's medium (DMEM), 2,7-dichlorofluorescein diacetate (DCFDA), 2,2,6,6-tetramethyl-4-piperidone (TEMP), ethidium bromide (EB), calf thymus (ct) DNA, agarose (molecular biology grade), and Annexin-V-FITC/PI kit were purchased from Sigma–Aldrich (U. S. A.) and used as received. The dipicolylamine (dpa), BODIPY-appended dpa (L^2) and diiodo-BODIPY-appended dpa (L^3) were synthesized following literature procedures.[29] Tetrabutylammonium perchlorate (TBAP), prepared by reacting tetrabutylammonium bromide and perchloric acid, was used for electrochemical experiments in small quantity (caution!). Mitotracker Deep Red (MTR), Lyso Tracker Deep Red (LTR) and fetal bovine serum (FBS) were procured from Invitrogen U.S.A.

The elemental analysis of the complexes was carried out using a Thermo Finnigan FLASH EA 1112 CHNS analyzer. The infrared (IR) and electronic spectra (UV-Vis, emission) were recorded with Bruker Alpha, Perkin–Elmer spectrum one 55 and Perkin–Elmer LS 55 fluorescence, spectrometers at room temperature. The fluorescence quantum yields of the compounds were obtained by a relative method as described in the literature.[52] Molar conductivity measurements were performed with a Control Dynamics (India) conductivity meter. Magnetic susceptibility measurements of the samples at 298K were carried out using a magnetic susceptibility balance of Sherwood Scientific, Cambridge (U. K.) using $Hg[Co(SCN)_4]$ as a standard. Cyclic voltammetric measurements were taken with an EG&G PAR model 253 VersaStat potentiostat/galvanostat with electrochemical analysis software 270 and a three electrode setup consisting of glassy carbon working, platinum wire auxiliary and a saturated calomel reference electrode (SCE) in DMF-0.1 M TBAP as the supporting electrolyte. Electrospray ionization (ESI) mass spectral measurements were carried out using an Agilent Technologies 6538 Ultra High definition accurate-mass Q-TOF LC/MS ESI model mass spectrometer. Flow cytometric analysis were performed using the Becton Dickinson (BD) FACS (fluorescence-activated cell sorting) Verse™ flow cytometer. Confocal microscopy cellular images were acquired from Leica TCS, SP5 microscope with oil immersion lens of 63X magnification. Iron contents in complexes **2** and **3** treated HeLa cells were measured by Perkin−Elmer Optima 7000 DV ICP-OES.

Synthesis of ligands: The dipicolylamine (dpa) derivatives of two BODIPY moieties were synthesized following procedures mentioned in the literature.[29b] The Schiff base ligands were synthesized by literature procedures.[29a] All the ligands were characterized by NMR and mass spectroscopy before preparing their metal complexes.

Synthesis of $[Fe(L^{1\text{-}3})(L^{4,5})](NO_3)$ (1 - 4): The complexes were synthesized following a general synthetic procedure where $Fe(NO_3)_3{\cdot}9H_2O$ (0.4 g, 1 mmol) was dissolved in 5 mL anhydrous methanol and dipicolylamine base (0.29 g bzdpa for **1**, 0.53 g L^2 for **2, 3**, 0.79 g L^3 for **4**) also dissolved in methanol was added dropwise under nitrogen atmosphere at room temperature. This reaction mixture was allowed to stir for 2 h. The Schiff base ligand $L^{4,5}$ (pyridoxal hydrochloride, 1 mmol, 0.26 g, for **1, 3, 4**; salicylaldehyde, 1 mmol, 0.21 g for **2**) was dissolved in 10 mL methanol and then deprotonated by treating with 2 eq. of triethylamine (0.2 g). This solution was then added to the reaction mixture and stirred for 3 h. The solution was filtered, concentrated and precipitated by addition of diethyl ether. The solid was isolated and washed with cold ethanol, and then finally dried in vacuum over P_4O_{10}.

$[Fe(L^1)(L^4)](NO_3)$ (**1**): Yield: 75%. Anal. Calcd for $C_{33}H_{31}FeN_6O_6$ (MW: 663.1642): C, 59.74; H, 4.71; N, 12.67. Found: C, 59.88; H, 4.59; N, 12.60. ESI-MS in MeOH (m/z): 601.1776 $[M-NO_3]^+$. IR data [cm^{-1}]: 2900 (br), 2358 (w), 1575 (m), 1384 (s), 1279 (vs), 1010 (m), 818 (w), 740 (vs), 565 (w) (vs, very strong; s, strong; m, medium; w, weak; br, broad.). UV-visible in 1:1 DMF:DPBS [λ_{max}/nm (ε/M^{-1} cm^{-1})]: 270 (46450), 386 sh (16025); Molar conductivity in 10% aqueous DMF at 298 K [Λ_M/S m^2 M^{-1}]: 77. μ_{eff} [μ_B] at 298 K: 5.86.

$[Fe(L^2)(L^5)](NO_3)$ (**2**): Yield: 30%. Anal. Calcd for $C_{45}H_{41}BF_2FeN_7O_5$ (MW: 864.5037): C, 62.52; H, 4.78; N, 11.34. Found: C, 62.57; H, 4.66; N, 11.53. ESI-MS in MeOH (m/z) 802.2702 $[M-NO_3]^+$. IR data [cm^{-1}]: 1625 (vs), 1341 (vs), 1282 (vs), 1157 (s), 1024 (m), 874 (w), 749 (s), 598 (w), 523 (w). UV-visible in 1:1 DMF:DPBS [λ_{max}/nm (ε/M^{-1} cm^{-1})]: 270 (47185), 400 sh (26420), 500 (42400) (sh, shoulder); Molar conductivity in 10% aqueous DMF at 298 K [Λ_M/S m^2 M^{-1}]: 69; μ_{eff} [μ_B] at 298 K: 5.83.

$[Fe(L^2)(L^4)](NO_3)$ (**3**): Yield: 30%. Anal. Calcd for $C_{46}H_{44}BF_2FeN_8O_6$ (MW: 909.2794): C, 60.74; H, 4.88; N, 12.32. Found: C, 60.96; H, 4.85; N, 12.65. ESI-MS in MeOH (m/z): 847.2916 $[M-NO_3]^+$. IR data [cm^{-1}]: 3000 (br), 1635 (w), 1577 (w), 1295 (vs), 1168 (m), 992 (m), 739 (m), 583(w). UV-visible in 1:1 DMF:DPBS [λ_{max}/nm (ε/M^{-1} cm^{-1})]: 265 (42130), 386 sh (24330), 500 (45100); Molar conductivity in 10% aqueous DMF at 298 K [Λ_M/S m^2 M^{-1}]: 71; μ_{eff} [μ_B] at 298 K: 5.82.

$[Fe(L^3)(L^4)](NO_3)$ (4): Yield: 20%. Anal. Calcd for $C_{46}H_{42}BF_2FeI_2N_8O_6$ (MW: 1161.3374): C, 47.57; H, 3.65; N, 9.64. Found: C: 46.98; H, 3.62; N, 9.92. ESI-MS in MeOH (m/z): 1099.0849 $[M-NO_3]^+$. IR data [cm^{-1}]: 3000 (br), 2354 (w), 1578

(m), 1389 (s), 1394 (s), 1294 (vs), 1156 (m), 992 (m), 820 (w), 751 (m), 518 (w). UV-visible in 1:1 DMF:DPBS [λ_{max}/nm (ε/M^{-1} cm^{-1})]: 265 (37455), 407 sh (25140), 532 (35520); Molar conductivity in 10% aqueous DMF at 298 K [Λ_M/S m^2 M^{-1}]: 73; μ_{eff} [μ_B] at 298 K: 5.85.

Theoretical Methods: The geometries of the complexes **1**, **3** and **4** were optimized by density functional theory (DFT) using B3LYP level of theory and LanL2DZ basis set as implemented in Gaussian 09 program.[34] The electronic transitions with their transition probability were obtained using linear response time dependent density functional theory (TDDFT).

Cellular experiments: The cancer cells HeLa, MCF7, and HepG2 and the immortalized non-cancer HPL1D cells were grown in 100 mm polymer culture dishes (SPL Life sciences, Korea) in DMEM supplemented with 10% FBS, 100 U penicillin/mL, 100 µg streptomycin/mL and incubated in a humidified 5% CO_2 incubator (Sanyo, UK) at 37 °C. "MTT Assay" was performed to understand the photocytotoxic effect of the complexes in these cell lines. For individual cell lines, ~8 x 10^3 cells were seeded in two 96 well plates in 100 µL medium per well and were grown for 24h at 37 °C in a CO_2 incubator. The complexes were dissolved in 1% DMSO and were added to the cells at different concentrations. Incubation was continued for another 4h. Thereafter, the medium of one plate was replaced with DPBS and photo-irradiated for 1h in broad-band visible light (400-700 nm) using a Luzchem Photoreactor (Model LZC-1, Ontario, Canada; light fluence rate: 2.4 mW cm^{-2}; light dose: 10 *J* cm^{-2}). This was followed by removal of DPBS and addition of fresh medium. The medium of the other plate was discarded and replaced with fresh medium. Both the plates were incubated for a further period of 20h in the dark which was followed by addition of 25 µL MTT (4 mg mL^{-1}) in each well and additional 3 h incubation in dark. Finally the culture medium was discarded from each well of the plates and 200 µL DMSO was added to each well to solubilize the purple formazan crystals. The absorbance at 540 nm was measured using a Molecular Devices Spectra Max M5 plate reader. The cytotoxicity of the complexes was measured as the percentage ratio of absorbance of treated cells to the untreated controls. The IC_{50} values were determined by nonlinear regression analysis (Graph Pad Prism 6).

For cellular incorporation assay, in 6-well plates ~0.3 x 10^6 cells were seeded per well and were grown for 24 h. Subsequently the cells were washed and incubated for 4 h in dark. The cells were then washed with PBS, trypsinized, re-suspended in PBS and acquired on the BD FACS Verse™ flow cytometer (BD Biosciences, USA). The cells were selected on the singlet gate (forward scatter-area versus forward scatter-height) and live gate (forward scatter-area versus side scatter-area) and ~10,000 events were recorded. The results were analyzed using the flow cytometry analysis software, FlowJo® (USA) and the histograms were constructed.[53] The experiment was repeated with cells that were pretreated with pyridoxal hydrochloride (2 mM) 4 h prior to treatment with the complexes. Dose-dependent estimation of cellular uptake study was performed to observe the effect of varying concentrations of VB_6 on the cellular uptake using flow cytometry.

DCFDA assay was performed for intracellular ROS estimation using the fluorogenic dye, 2'7'-dichlorofluorescein diacetate (DCFDA, 287810, Calbiochem®, USA). The cells were seeded in 6 wells plate and incubated for 24 h. Subsequently, the cells were treated with the compounds for 4 h at 37 °C in dark and then photo-exposed for 1 h. Post exposure, the cells were washed, trypsinized and re-suspended in DMEM medium. Viable cell numbers were enumerated by Trypan blue exclusion assay using a hemocytometer. About 0.25 x 10^6 viable cells were stained with 10 µM of DCFDA and incubated at 37 °C for 30 min in dark. Next, the cells were washed, re-suspended in PBS and acquired (10,000 cells in the live singlet gate) on the BD FACS Verse™ flow cytometer (BD Biosciences, USA). The results were analyzed and the representative histograms were constructed using the flow cytometry analysis software, FlowJo® (USA)[54].

For quantification of cellular iron by ICPMS, ~1x10^5 HeLa cells were grown in 35 mm culture dishes in DMEM supplemented with 10% FBS. The complexes **2** and **3** were dissolved in DMSO in their IC_{50} concentrations and added to the cells and incubated for 4 h. The culture medium was then discarded, cells were trypsinized and washed with cold DPBF. The cell pellets were prepared by spinning them down at 1000 rpm for 10 min. Subsequently, the pellets were digested with 70% HNO_3 at 65 °C for 2 h followed by a dilution to a final concentration of 2% nitric acid. The iron content was then measured using the spectrometer previously calibrated with standard ferric nitrate solutions.

In Annexin V / Propidium iodide (PI) Assay, the cells were stained with Annexin V-FITC and PI. The cells were seeded in 6-well plates and incubated for 24 h, post which, the cells were washed and treated with the mentioned compounds for 4 h at 37°C in dark followed by photo-exposure for 1 h. The cells were subsequently washed, trypsinized and resuspended in DMEM medium. The viable cells were enumerated by Trypan blue exclusion assay using a hemocytometer and ~0.25 x 10^6 viable cells were stained with Annexin V-FITC and PI, according to the manufacturer's instructions (APOAF, Sigma-Aldrich, USA). The cells were acquired (10,000 events in the singlet gate) on the BD FACS Verse™ flow cytometer (BD Biosciences, USA) and the BD FACSDiva™ software was used to analyze, construct the Annexin V-FITC versus PI dot-plots and quantify the results.

The cellular localization pattern of the fluorescent complex **3** (10 µM) in HeLa cells was visualized using a confocal microscope. Standard experimental procedures were adopted for cell plating and post treatment processing.[38] To understand the sub-cellular localization of the complex, HeLa cells were incubated with 10 µM of complex for 4 h in dark. Post incubation, the medium was discarded and the cells were washed thrice with DPBS. Lyso Tracker Red (250 nM) was added to the cells and incubated for 10 min at room temperature. The live cells

were then directly imaged under a confocal microscope (TCS SP5, Leica, Germany) using 63X HCX APO L U-V-I water immersion objective (NA 0.9).

DNA binding and cleavage experiments: DNA binding constants of the complexes were obtained from UV-visible spectral studies using calf thymus (ct) DNA by the reported procedures.[55] The DNA photocleavage activity of the complexes was studies using supercoiled (SC) pUC19 plasmid on light irradiation using diode lasers and by gel electrophoresis. A continuous-wave (CW) diode laser made of Research Electro-Optics, Colorado; (U. S. A.), model no. EXLSR-532-100-CDRH was used as a monochromatic visible light of 532 nm (100 mW power, 1 h exposure time, 0.32 ± 0.02 mm beam diameter). External agents, *viz*., sodium azide and TEMP (2,2,6,6-tetramethyl-4-piperidone) as singlet oxygen quenchers and DMSO, KI and catalase as hydroxyl radical scavengers and superoxide dismutase (SOD) as a superoxide scavenger were used for mechanistic studies to determine the nature of the ROS generated using procedures that are reported earlier.[37]

Supporting Information (see footnote on the first page of this communication): General synthetic scheme of ligands and complexes (Scheme S1), Coordinates from DFT study (Tables S1-S4), ESI-MS spectra (Figures S1-S4), IR spectra (Figure S5), cyclic voltammograms (Figures S6,S7), Energy optimized geometry and HOMO–LUMO diagram of complex **2** (Figure S8), Stability plots for ligands (Figure S9), Stability plots for complexes (Figure S10), Singlet oxygen quantum yield plot (Figure S11), MTT assay bar diagram (Figure S12), Concentration vs % cell viability MTT plots (Figures S13-S16), time dependent incorporation studies (Figure S17), effect of Vitamin B_6 pre-saturation on incorporation (Figure S18), Annexin assay for complex **4** (Figure S19), DPBF decay plot for complex **3** (Figure S20), DNA binding MVH plots (Figure S21), and gel electrophoresis diagrams (Figures S22-S24).

Acknowledgements

We thank the Department of Science and Technology (DST), Government of India, for financial support (SR/S5/MBD-02/2007, EMR/2015/000742). A.R.C. thanks DST for J.C. Bose national fellowship. We thankfully acknowledge the supports of the DBT-IISc partnership program, the Bio-imaging and the flow cytometry facility Division of Biological Sciences, IISc. We thank Vasista Adiga from the Center for Infectious Diseases Research (CIDR) for helping with FACS analysis. The authors also thank the Alexander von Humboldt Foundation for donation of an electroanalytical system.

Keywords: Bioinorganic chemistry • Iron • Antitumor agents • Borondipyrromethene derivatives • Vitamin B6

References

[1] (a) J. Liu, C. Jin, B. Yuan, Y. Chen, X. Liu, L. Jia, H. Chao, *Chem. Commun.* **2017**, *53*, 9878-9881; b) N. C. Fan, F. Y. Cheng, J. A. Ho, C. S. Yeh, *Angew. Chem., Int. Ed.* **2012**, *51*, 8806−8810; c) F. Ménard, V. Sol, C. Ringot, R. Granet, S. Alves, C. Morvan, Y. Le Queneau, N. Ono, P. Krausz, *Bioorg. Med. Chem.* **2009**, *17*, 7647−7657; d) S. Hirohara, M. Obata, S. I. Ogata, C. Ohtsuki, S. Higashida, S. I. Ogura, I. Okura, M. Takenaka, H. Ono, Y. Sugai, Y. Mikata, M. Tanihara, Y. Masao, S.J. Yano, *Photochem. Photobiol. B* **2005**, *78*, 7−15; e) O. Hocine, M. Gary-Bobo, D. Brevet, M. Maynadier, L. Raehm, S. Richeter, B. Loock, A. Morère, P. Maillard, M. Garcia, J.O. Durand, *Int. J. Pharm.* **2012**, *423*, 509−515.

[2] a) C. Frochot, B. Di Stasio, M. Barberi-Heyob, M.C. Carre, J.M. Zwier, F. Guillemin , M.L. Viriot *Oftalmologia.* **2003**, *56*, 62–66; b) J. Gravier, R. Schneider, C. Frochot, T. Bastogne, F. Schmitt, J. Didelon, F. Guillemin, M. Barberi-Heyob *J. Med. Chem.* **2008**, *51* , 3867–3877.

[3] a) W. Xia, P.S. Low *J. Med. Chem.* **2010***, 53*, 6811–6824; b) R.J. Lee, P.S. Low *J. Biol. Chem.* **1994,** *269*, 3198–3204.

[4] a) R. Spector, C.E. Johanson, *J. Neurochem.* **2007**, *103,* 425–438; b) S. Pandey, P. Garg, S. Lee, H.W. Choung, Y.H. Choung, P.H. Choung, J.H. Chung, *Biomaterials* **2014**, *35*, 9332–9342.

[5] a) J. Stolz, M. Vielreicher, *J. Biol. Chem.* **2003,** *278*, 18990–18996; b) H. Hellman, S. Mooney, *Molecules* **2010**, *15,* 442–459.

[6] a) S. Mooney, J.E. Leuendorf, C. Hendrickson, H. Hellmann, *Molecules* **2009**, *14*, 329–351; b) G. Giardina, P. Brunotti, A. Fiascarelli, A. Cicalini, M.G.S. Costa, A.M. Buckle, M.L.D. Salvo, A. Giorgi, M. Marani, A. Paone, S. Rinaldo, A. Paiardini, R. Contestabile, F. Cutruzzola, FEBS J. **2015**, 282, 1225–1241.

[7] S. Banerjee, A. Dixit, R.N. Shridharan, A. A. Karande, A. R. Chakravarty, *Chem. Commun*. **2014**, *50*, 5590−5592.

[8] S. Banerjee, A. Dixit, A. A. Karande, A. R. Chakravarty *Dalton Trans.* **2016**, *45*, 783–796.

[9] K. Szacilowski, W. Macyk, A. Drzewiecka-Matuszek, M. Brindell, G. Stochel, *Chem. Rev.* **2005**, *105*, 2647−2694.

[10] R. M. Burger, S. J. Projan, S. B. Horwitz, J. Peisach, *J. Biol. Chem.* **1986**, *261*, 15955–15959.

[11] a) T. Kowada, H. Maeda , K. Kikuchi, *Chem. Soc. Rev.* **2015**, *44*, 4953–4972; b) S. H. Lim, C. Thivierge, P. N. Sliwinska, J. Han, H. van den Bergh, G. Wagnieres, K. Burgess, H. B. Lee, *J. Med. Chem.* **2010**, *53*, 2865–2874.

[12] a) X. Li, S. Kolemen, J. Yoon, E.U. Akkaya, *Adv. Funct. Mater.* **2017**, *27*, 1604053; b) T. Ozdemir, J. L. Bila, F. Sozmen, L. T. Yildirim, E. U. Akkaya, *Org. Lett.* **2016**, *18*, 4821–4823; c) A. Turksoy, D. Yildiz, E.U. Akkaya, *Coord. Chem. Rev.* **2017**, https://doi.org/10.1016/j.ccr.2017.09.029

[13] a) X. Wang, Z. Guo, *Chem. Soc. Rev.* **2013**, *42*, 202−224; b) J. J. Wilson, S. J. Lippard, *Chem. Rev.* **2014**, *114*, 4470−4495.

[14] a) M. Gosland, B. Lum, J. Schimmelpfennig, J. Baker, M. Doukas, *Pharmacotherapy* **1996**, *16*, 16–39; b) C. Jacobsen, F. Honeck, *Andrology* **2015**, *3*, 111–121; c) K. Barabas, R. Milner, D. Lurie, C. Adin, *Vet. Comp. Oncol.* **2008**, 6, 1–18; d) S. D'Aguanno, A. D'Alessandro, L. Pieroni, A. Roveri, M. Zaccarin, V. Marzano, M. De Canio, S. Bernardini, G. Federici, A. Urbani *J. Proteome Res.* **2011**, *10*, 416–428; e) M. Wachowska, A. Muchowicz, J. Golab, *Front. Oncol*. **2015**, *5* , 176.

[15] a) A. Juarranz, P. Jaen, F. Sanz-Rodríguez, J. Cuevas, S. González, *Clin. Transl. Oncol.* **2008**, *10*, 148–154; b) D. van Straten, V. Mashayekhi, H. S. de Bruijn, S. Oliveira, D. J. Robinson *Cancers* **2017**, *9*, 1–54.

[16] I.J. Macdonald, T.J. Dougherty, *J. Porphyr. Phthalocyanins* **2001**, *5* , 105–129.
[17] a) S. Chakrabortty, B. K. Agrawalla, A. Stumper, N. M. Vegi, S. Fischer, C. Reichardt, M. Kögler, B. Dietzek, M. Feuring-Buske, C. Buske, S. Rau, T. Weil, *J. Am. Chem. Soc.* **2017**, *139* , 2512–2519; b) W. Zhou, X. Wang, M. Hu, C. Zhu, Z. Guo, *Chem. Sci*. **2014***, 5,* 2761–2770; c) T. Sun, X. Guan, M. Zheng, X. Jing, Z. Xie, *ACS Med. Chem. Lett.* **2015**, *6*, 430−433; d) K. Mitra, S. Gautam, P. Kondaiah, A. R. Chakravarty, *ChemMedChem* **2016**, *11*, 1956−1967.
[18] H. Huang, B. Yu, P. Zhang, J. Huang, Y. Chen, G. Gasser, L. Ji, H. Chao, *Angew. Chem. Int. Ed.* **2015**, *54*, 14049–14052.
[19] S. Marrachea, R. K. Pathak, S. Dhar, *PNAS* **2014**, *111,* 10444–10449.
[20] M. Millard, J.D. Gallagher, B.Z. Olenyuk, N. Neamati, *J. Med. Chem.* **2013** , *56*, 9170–9179.
[21] S. H. van Rijt, I. Romero-Canelón, Y. Fu, S. D. Shnyder, P. J. Sadler *Metalllomics* **2014**, *6*, 1014–1022.
[22] a) T. Gao, H. He, R. Huang, M. Zheng, F.-F. Wang, Y.-J. Hu, F.-L. Jiang, Y. Liu, *Dyes Pigm.* **2017,** *141*, 530-535; b) S. Zhang, T. Wu, J. Fan, Z. Li, N. Jiang, J. Wang, B. Dou, S. Sun, F. Song, X. Peng, *Org. Biomol. Chem.* **2013,** *11,* 555-558.
[23] A. Garai, I. Pant, A. Bhattacharyya, P. Kondaiah, A. R. Chakravarty, *ChemistrySelect* **2017**, *2*, 11686-11692.
[24] T. M. Tsubone, W. K. Martins, C. Pavani, H. C. Junqueira, R. Itri, M. S. Baptista, *Sci. Rep.* **2017**, *7,* 6734.
[25] M. Domenech, I. Marrero-Berrios, M. Torres-Lugo, C. Rinaldi, *ACS Nano* **2013**, *7*, 5091–5101.
[26] W. Hu, H. Ma, B. Hou, H. Zhao, Y. Ji, R. Jiang, X. Hu, X. Lu, L. Zhang, Y. Tang, Q. Fan, W. Huang, *ACS Appl. Mater. Interfaces* **2016**, *8*, 12039–12047.
[27] M. Li, R. Tian, J. Fan, J. Du, S. Long, X. Peng *Dyes Pigm.* **2017**, 147, 99-105.
[28] D.-Y. Zhang, Y. Zheng, C.-P. Tan, J.-H. Sun, W. Zhang, L.-N. Ji, Z.-W. Mao *ACS Appl. Mater. Interfaces,* **2017**, *9*, 6761−6771.
[29] a) U. Basu, I. Pant, A. Hussain, P. Kondaiah, A. R. Chakravarty, *Inorg. Chem.* **2015**, *54*, 3748−3758; b) A. Bhattacharyya, A. Dixit, K. Mitra, S. Banerjee, A. A. Karande, A. R. Chakravarty, *Med. Chem. Commun.* **2015**, *6*, 846–851.
[30] a) D. A. Tekdaş, G. Viswanathan, S. Z. Topal, C. Y. Looi, W. F. Wong, G. M. Y. Tan, Y. Zorlu, A. G. Gürek, H. B. Lee, F. Dumoulin, *Org. Biomol. Chem.* **2016**, *14*, 2665–2670; b) S. Ji, J. Ge, D. Escudero, Z. Wang, J. Zhao, D. Jacquemin, *J. Org. Chem.* **2015**, *80*, 5958–5963.
[31] F. A. Miller, C. H. Wilkins, *Anal. Chem.* **1952**, *24,* 1253-1294.
[32] J. Bañuelos, F. L. Arbeloa, V. Martínez, I. L. Arbeloa, *Chem. Phys.* **2004**, *296*, 13–22.
[33] a) M. Velusamy, M. Palaniandavar, *Inorg. Chem.* **2003**, *42*, 8283−8293; b) M. Palaniandavar, M. Velusamy, R. Mayilmurugan, *J. Chem. Sci.* **2006**, *118*, 601−610.
[34] a) A. D. Becke, *Phys. Rev. A* **1988**, *38*, 3098–3100; b) W. R. Wadt, P. J. Hay, *J. Chem. Phys.* **1985**, *82*, 284–298; c) M. J. Frisch, G. W. Trucks, H. B. Schlegel, G. E. Scuseria, M. A. Robb, J. R. Cheeseman, G. Scalmani, V. Barone, B. Mennucci, G. A. Petersson, H. Nakatsuji, M. Caricato, X. Li, H. P. Hratchian, A. F. Izmaylov, J. Bloino, G. Zheng, J. L. Sonnenberg, M. Hada, M. Ehara, K. Toyota, R. Fukuda, J. Hasegawa, M. Ishida, T. Nakajima, Y. Honda, O. Kitao, H. Nakai, T. Vreven, J. A. Montgomery Jr., J. E. Peralta, F. Ogliaro, M. Bearpark, J. J. Heyd, E. Brothers, K. N. Kudin, V. N. Staroverov, R. Kobayashi, J. Normand, K. Raghavachari, A. Rendell, J. C. Burant, S. S. Iyengar, J. Tomasi, M. Cossi, N. Rega, J. M. Millam, M. Klene, J. E. Knox, J. B. Cross, V. Bakken, C. Adamo, J. Jaramillo, R. Gomperts, R. E. Stratmann, O. Yazyev, A. J. Austin, R. Cammi, C. Pomelli, J. W. Ochterski, R. L. Martin, K. Morokuma, V. G. Zakrzewski, G. A. Voth, P. Salvador, J. J. Dannenberg, S. Dapprich, A. D. Daniels, Ö. Farkas, J. B. Foresman, J. V. Ortiz, J. Cioslowski, D. J. Fox, *Gaussian 09, Revision A.02*, Gaussian, Inc., Wallingford CT, 2009.
[35] U. Basu, I. Khan, A. Hussain, B. Gole, P. Kondaiah, A. R. Chakravarty, *Inorg. Chem.* **2014**, *53*, 2152−2162.
[36] U. Basu, I. Khan, A. Hussain, P. Kondaiah, A. R. Chakravarty *Angew. Chem. Int. Ed.* **2012**, *51*, 2658 –2661.
[37] A. Garai, U. Basu, I. Khan, I. Pant, A. Hussain, P. Kondaiah, A. R. Chakravarty, *Polyhedron* **2014**, *73*, 124−132
[38] S. Saha, R. Majumdar, A. Hussain, R. R. Dighe, A. R. Chakravarty, *Philos. Trans. R. Soc. A* **2013**, *371*, 20120190.
[39] E. Delaey, F. Van Laar, D. De Vos, A. Kamuhabwa, P. Jacobs, P. De Witte, *Photochem. Photobiol. B Biol.* **2000**, *55*, 27–36.
[40] K. Mitra, U. Basu, I. Khan, B. Maity, P. Kondaiah, A. R. Chakravarty, *Dalton Trans.* **2014**, *43*, 751−763.
[41] M. Olivo, R. Bhuvaneswari, S. S. Lucky, N. Dendukuri, P. S. P. Thong, *Pharmaceuticals (Basel)* **2010**, *3*, 1507–1529.
[42] S. R. Denmeade, X. S. Lin, J. T. Isaacs, *The Prostrate* **1996**, *6*, 251–265.
[43] a) D. E. Dolmans, D. Fukumura, R. K. Jain, *Nat. Rev. Cancer* **2003**, *3*, 381–387; b) M. Issa, M. Manela-Azulay, *An. Bras. Dermatol.* **2010**, *85*, 501–511.
[44] J. T. F. Lau, P.-C. Lo, X.-J. Jiang, Q. Wang, D. K. P. Ng, *J. Med. Chem.* **2014**, *57*, 4088–4097.
[45] A. Bhattacharyya, A. Dixit, S. Banerjee, B. Roy, A. Kumar, A. A. Karande , A. R. Chakravarty, *RSC Adv.* **2016**, *6*, 104474–104482.
[46] a) N. Gandra, A. T. Frank, O. Le Gendre, N. Sawwan, D. Aebisher, J. F. Liebman, K. N. Houk, A. Greer, R. Gao, *Tetrahedron* **2006**, *62*, 10771–10776; b) N. Adarsh, M. Shanmugasundaram, R. R. Avirah, D. Ramaiah, *Chem.–Eur. J.* **2012**, *18*, 12655–12662; c) A. P. Thomas, P. S. S. Babu, S. A. Nair, S. Ramakrishnan, D. Ramaiah, T. K. Chandrashekar, A. Srinivasan, M. R. Pillai, *J. Med. Chem*. **2012**, *55*, 5110−5120.
[47] M. Leist, M. Jäättelä, *Nat. Rev. Mol. Cell. Biol.* **2001**, *2*, 589–598.
[48] a) M-T. Gyparaki, A. G. Papavassiliou, *Trends Mol. Med.* **2014**, *20*, 239−241; b) H. Lee, D. H. M. Dam, J. W. Ha, J. Yue, T. W. Odom, *ACS Nano* **2015**, *9*, 9859–9867.
[49] P. Boya, G. Kroemer, *Oncogene* **2008**, *27*, 6434−6451.
[50] A. U. Khan, *J. Phys. Chem.* **1976**, *80*, 2219–2227.
[51] D. D. Perrin, W. L. F. Armarego and D. R. Perrin, Purification of Laboratory Chemicals, Pergamon Press, Oxford, **1980**.
[52] A. T. R. Williams, S. A. Winfield, J. N. Miller, *Analyst* **1983**, *108*, 1067–1071.
[53] N. Mukherjee, S. Podder, S. Banerjee, S. Majumdar, D. Nandi, A. R. Chakravarty, *Eur. J. Med. Chem.* **2016** , *122*, 497–509.
[54] a) L.A. Herzenberg, J. Tung, W. A. Moore, L. A. Herzenberg, D. R. Parks, *Nat Immunol*. **2006**, *7*, 681–685; b) D. R. Parks, M. Roederer, W. A. Moore, *Cytometry A*. **2006**, 6, 541–551.
[55] a) J. D. McGhee, P. H. Von Hippel, *J. Mol. Biol. 1974*, *86,* 469–489; b) M. T. Carter, M. Rodriguez, A. J. Bard, *J. Am. Chem. Soc.* **1989**, *111*, 8901–8911.

10.1002/ejic.201701487

WILEY-VCH

FULL PAPER

Ternary iron(III) complexes of *NNN*-donor ligands having pendant BODIPY moieties and *O,N,O*-donor vitamin-B6 Schiff base showed singlet oxygen induced photo-cytotoxicity in the cancer cells with apoptotic cell death and lysosomal localization from imaging studies. The complexes displayed higher cellular uptake in the cancer cells compared to normal cells.

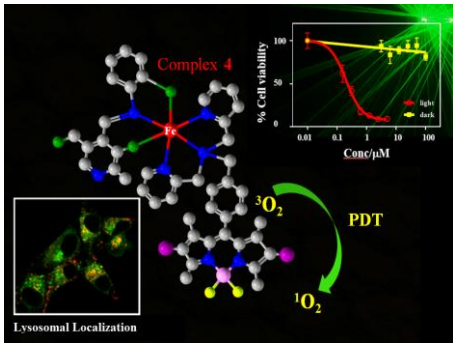

Key Topic*: Photodynamic Therapy

Somarupa Sahoo, Santosh Podder, Aditya Garai, Shamik Majumdar, Nandini Mukherjee, Uttara Basu, Dipankar Nandi*, Akhil R. Chakravarty*

Page No. – Page No.

Title:

Iron(III) Complexes of Vitamin-B6 Schiff Base with Borondipyrro-methene Pendants for Lysosome Selective Photocytotoxicity